On the Latent Heat Release in a Cyclone Crossing the Rocky Mountains

By
Herbert Riehl and William Gray

Department of Atmospheric Science
Colorado State University
Fort Collins, Colorado

A report on laboratory work carried out during the course "The Atmosphere and the Water Cycle" conducted in the winter quarter of 1961-62 under a grant from the National Science Foundation to Colorado State University

July 1962

Colorado State University

Department of Atmospheric Science

Paper No. 533

ON THE LATENT HEAT RELEASE IN A CYCLONE CROSSING THE ROCKY MOUNTAINS

by

Herbert Riehl

and

William Gray

A report on laboratory work carried out during the course
"The Atmosphere and the Water Cycle"
conducted in the winter quarter of 1961-62 under a grant from the
National Science Foundation to Colorado State University

Technical Paper No. 35
Department of Atmospheric Science
Colorado State University
Fort Collins, Colorado

July 1962

ON THE LATENT HEAT RELEASE IN A CYCLONE CROSSING THE ROCKY MOUNTAINS

by

Herbert Riehl

and

William Gray

Abstract

At first the water vapor balance is computed for a cyclone crossing the Rocky Mountains 1-2 April 1957 in a coordinate system moving with the cyclone. In this coordinate system the surface pressure varies strongly due to the variable height of the underlying terrain.

Next precipitation is computed in the same coordinate system and compared with precipitation from rain and snow gauge measurements. It is found that the left front sector of the cyclone produces most precipitation just as in cyclones elsewhere and that computed exceeded observed precipitation by about 50 per cent; this may be due to lack of precipitation stations at high altitudes. Total water yield for the storm of moderate intensity is large, and it is seen that only a few such storms are needed to produce the average annual runoff from one of the major western river systems.

Next a model is introduced which assumes active ascent in 10 per cent of the precipitation area, concentrated mainly along the upslope portions of the precipitating sector. For such ascent the atmosphere was thermodynamically neutral or unstable in that sector. Given undilute ascent the temperature at which given fractions of the total condensate occurred can be computed. It is shown that over half of the condensation took place at temperatures where active freezing nuclei are scarce so that, for snow formation, considerable ascent of the supercooled water or seeding with ice nuclei from above would have to have taken place in order for the bulk of the condensed water to fall out in form of snow.

Finally, a computation was made of the release of kinetic energy due to ascent of warm precipitating air and descent of cold air within the confines of the cyclone core. It is shown that kinetic energy was released at a rate sufficient to regenerate the total energy of the cyclone in 24 hours. This energy generation amounted to seven per cent of the latent heat release. It is noted that the total temperature gradient in the middle troposphere across the cyclone had the same amount as the difference between dry- and moist adiabatic ascent in the precipitating sector. Hence, even under the conditions of general low moisture content as encountered in a storm over the Rockies compared to one over the eastern United States or over the oceans, a model with ascent neglecting precipication would rapidly run down the generation of kinetic energy to nothing and fail as a predictor.

Introduction

There is unanimous agreement that one of the major problems facing the western United States is maximum utilization of the scant water resources. Improved understanding of the precipitation process in this area would contribute toward the solution of problems relating to water supply. A major fraction of the precipitation measured in any season comes from a few well organized storm systems. About six such systems may account for as much as half of the precipitation of a water year. It is of interest to make computations on the precipitation yield from such a disturbance, with emphasis on the following questions:

(1) What is the precipitation pattern with respect to the cyclone?

(2) Can precipitation be computed with sufficient accuracy from the convergence of moisture flux plus local changes following the center?

(3) If so, how do the calculated amounts agree with those obtained from rain and snow gauge measurements?

(4) At what temperatures does condensation take place? Are these temperatures low enough to insure the presence of active natural freezing nuclei?

(5) What are the energy sources and conversions that drive the storm? Can the contribution of release of condensation heat be traced and computed?

(6) How do the observed characteristics of cyclones over the Rockies compare with present ideas about cyclone dynamics?

Solution of all of these questions will require much serious effort. For purposes of preliminary orientation, especially on methodology and computational procedures, a cyclone study was made part of the laboratory work in a course entitled "The Atmosphere and the Water Cycle" offered during the winter of 1961-62. An intense though not extreme cyclone was investigated which passed across the southern Rocky Mountains during the period 1-3 April 1957; this cyclone remained approximately in steady state.

Data and Reference System

The observations mainly consisted of rawinsonde observations taken twice daily by the United States Weather Bureau. Figs. 1-2 show the station locations and the density of the available network. The observations yield pressure, temperature, relative humidity, wind direction and wind speed as a function of height. Information on pressure is given by stating the height z_p at which a given pressure value occurs. The coded rawinsonde message gives the above information at certain standard pressure surfaces and, in addition, at significant levels where temperature and/or humidity have abrupt changes from the normal vertical distribution. Besides the rawinsonde data and a few available pilot balloon wind observations, precipitation observations were obtained from the compiled Climatological Data published by the United States Weather Bureau.

Fig. 3 shows the track of the 500-mb center during the period of study. The rate of center displacement was 18 knots at the beginning and slowed to 9 knots at the end. A box with side of 400 n.mi. was chosen as the area for computation. This box was centered on the 500-mb cyclone and oriented so that at each rawinsonde observation time one pair of sides was normal, the other pair parallel, to the direction of storm propagation. Therefore, the box was rotated in space during the period of study.

As indicated in fig. 3 the large box was subdivided into four smaller boxes, located right front, right rear, left front and left rear with respect to the storm center, looking down the direction of propagation. This arrangement was chosen because, from previous knowledge of cyclones, it should yield the major asymmetries of motion, precipitation and energy conversion about the center. The length of 200 n.mi. for the side of the small boxes, hence also the length of 400 n.mi. for the length of the large box, was determined by the fact that 200 n.mi. is the average distance between rawinsonde stations, therefore the smallest distance over which computations with fair reliability could be performed in most instances.

Fig. 4 gives more detail on the box and the coordinates fixed with respect to it. Dots show the locations at which values for flux calculations were tabulated. These dots were placed so that the values read there were taken as means over a distance of 100 n.mi. This was considered sufficient for our purposes and in keeping with the significance of detail to be expected from analyses based on the spacing of upper-air stations. The coordinate system chosen was s, n, p, t, where fig. 4 shows the s- and n-axes,

p is pressure and t time. In this quasi-Lagrangian coordinate system the horizontal velocity components are u and v, positive along s and n. The 'vertical' component is given by $\omega \equiv dp/dt$.

Periods for computation were 1 April 0300 GMT (Greenwich Mean Time), 1 April 1500 GMT, 2 April 0300 GMT, 2 April 1500 GMT and 3 April 0300 GMT. At first, rawinsonde and pilot balloon observations for these periods were collected for the western United States. These observations were then plotted on tephigrams for thermodynamic analysis (cf. fig. 6). Wind data were also tabulated on the tephigrams. For the pilot balloon stations, winds were plotted against pressure to make them comparable with the rawin observations.

A particular feature of this analysis is the traverse of the cyclone over mountainous terrain. For computations under such circumstances the topographic features must be delineated to a significant degree, avoiding however the many details of the actual topography. Such details would be wanted only in studies of effects of mountain ranges on the meso-scale, toward which neither our problem nor our data were directed. Sangster (1960) has given an approximation of the topography well suited for our purposes. This topography, converted to pressure with use of the standard atmosphere, is shown in fig. 5. While the cyclone center moved at relatively constant pressure, portions of the box grid moved up and down large distances.

Method for Computing Precipitation Following Center

A precipitation map portrays the pattern of rain or snowfall during a given time interval, such as a day, as different portions of a storm pass over the area of the map. For insight into the mechanisms producing precipitation it is necessary to construct a different kind of map, one which describes how precipitation is distributed with respect to the cyclone core. For this purpose we shall compute precipitation in each of the four small boxes of fig. 4. Let P denote precipitation rate and E evaporation rate over the area of one of the boxes, and let the moisture content of the cyclone remain constant for the present. Then

$$P - E = -\iint \rho \, q \, c_{nr} \, \delta \sigma - \lambda \, , \qquad (1)$$

where ρ is density, q specific humidity, c_{nr} the wind component in the relative coordinate system normal to the boundaries of the box taken positive outward, σ the vertical surface of the box extending from the ground to the top of the atmosphere and λ net transport of liquid or frozen water through the boundaries. In view of the size of the boxes, λ must be very small compared to P and may be neglected; even its sign is uncertain. The same holds for E when time increments of 12 or 24 hours are considered, since precipitation occurs rapidly over short time periods whereas evaporation proceeds slowly but continuously. Thus

$$P = -\iint \rho \, q \, c_{nr} \, \delta \, \sigma \, . \tag{2}$$

The right side of (2) denotes the net flux of water vapor in or out of the box. For correct computation, it is most important that the law of conservation of atmospheric mass is observed as a side condition. Evaluating between the surface pressure p_o and the pressure p_H at the top of the storm,

$$0 = \int \delta \ell \int_{p_o}^{p_H} c_{nr} \, \frac{\delta p}{g} \, . \tag{3}$$

Here g is the acceleration of gravity and $\delta \ell$ the element of horizontal circumference of the box. After establishing a field of c_{nr} (p, ℓ) so that (3) is satisfied, the lateral water vapor transport can be computed by evaluating (2) around the circumference of the box and over successive layers with constant pressure increment Δp above the top of the mountains and with variable pressure increments lower down. For one such layer the water vapor flux w_h, positive outward, is best evaluated from

$$w_h = \int \delta \ell \int q \, c_{nr} \, \frac{\Delta p}{g} \, , \tag{4}$$

where the hydrostatic equation has been used to introduce the pressure as coordinate explicitly. If Δp is chosen sufficiently small, we may replace the product $q \, c_{nr}$ by the mean value of each quantity over the pressure depth Δp. Designating $q \, \Delta p/g = m_w$, the total mass of water vapor per unit horizontal area in the column extending from p to $p + \Delta p$, the flux of vapor is

$$w_h = \int m_w \hat{c}_{nr} \, \delta\ell \, , \tag{5}$$

where the hat denotes averaging over Δp. The water vapor flux W_h across the entire boundary of the cyclone

$$W_h = \frac{\Sigma}{\Delta p} \int m_w \hat{c}_{nr} \, \delta\ell + \frac{\Delta p_o}{\Delta p} \int m_w \hat{c}_{nr} \, \delta\ell \, , \tag{6}$$

where Δp_o denotes the thickness of the layer nearest the ground. Numerically,

$$W_h = \frac{\Sigma}{\Delta p} \left[\sum_{N=4} m_w^i \hat{v}_n^i L + \sum_{N=4} m_w^i (\hat{u} - c)_n^i L \right] + \frac{\Delta p_o}{\Delta p} \left[\begin{array}{c} \text{as on} \\ \text{left} \end{array} \right], \tag{7}$$

In this expression L is the distance of 100 n.mi. over which one gridpoint of fig. 4 is considered to yield the weighted mean value; the subscript 'n' denotes that the proper sign convention of the horizontal velocity components with respect to the box must be observed; and the superscript 'i' refers to the gridpoints of fig. 4.

In practice Δp may be taken as 100 mb. When the integration is extended from a fixed lower pressure essentially coinciding with the ground to the top of the troposphere, the calculation is completed with evaluation of (7) since, in that case, $P = -W_h$. Bradbury (1957), Palmén (1958, 1962), Riehl (1959), Riehl and Byers (1960) and others have made computations of this type for the eastern United States, the West Indies and other areas of the globe except that these calculations were made in fixed rather than moving coordinate systems. Comparison with the precipitation measured at the ground, when available, was reasonably satisfactory. This indicates that atmospheric upper-air data are good enough for direct precipitation calculations provided that time and space increments are chosen properly.

Because of the low moisture content of the high troposphere and the difficulty of measuring humidity at very low temperatures, it usually suffices to terminate the calculation of (6) at a suitably chosen pressure surface. For winter cyclones over the Rockies it is very probable that the 400-mb surface

is a suitable terminal level. Nevertheless, the upward or downward moisture transport across this surface should be evaluated, as best possible, for verification.

This transport W_p across a constant-pressure surface, positive toward lower pressure, is given by

$$W_p = -\frac{1}{g}\int q\omega \, \delta A \, , \tag{8}$$

where A is the area of the box on the constant-pressure surface, in practice almost exactly the horizontal area. W_p may be evaluated by calculating the product $q\omega$ over a grid laid across the area. In our case, since the box with side of 200 n.mi. was the smallest unit of computation, W_p in the first approximation will be

$$W_p = -\frac{1}{g}\,\bar{q}\,\bar{\omega}\,A \, , \tag{9}$$

where the bar indicates averaging over the area. Since $-\omega A/g = M_p$, the mass flow across the constant-pressure surface, positive toward lower pressure, we can also write

$$W_p = \bar{q}\,\overline{M_p} \, . \tag{10}$$

An improvement over this computational procedure will be offered later. It is not important, however, at 400 mb where the moisture content of the air is very low and fluctuates only slightly over the area.

Up to now we have proceeded with the assumption that the moisture content of the cyclone remains constant. This assumption may be questioned for all cyclones in view of the life cycle from warm sector to occluded stage. Here, however, the change following the system may be small compared with convergence of transport. In our case the assumption must be invalid since the cyclone moved over terrain of variable elevation, hence its total mass changed with time. We must, therefore, compute the time derivative.

Per unit horizontal surface, this time derivative is given by $\delta/\delta t\left[\int q\ \Delta p/g\right]$, where both q and $\Delta p/g$ are variables. Further, the mass change of the cyclone is $\delta/\delta t \iint \delta p/g\ \delta A$, so that the equation of mass continuity

$$-\frac{1}{g}\frac{\delta \overline{p_o}}{\delta t} A = \int \delta \ell \int c_{nr} \frac{\delta p}{g} \tag{11}$$

after integration from a fixed upper pressure to a variable surface pressure. With these relations, the change of moisture following the cyclone, including all layers of the troposphere, is best computed by evaluating at first the total moisture content M_w at each computation period, given by

$$M_w = \int \delta A \int_{p=400}^{p_o} q \frac{\Delta p}{g} . \tag{12}$$

Then the precipitation rate

$$P = -\frac{\delta M_w}{\delta t} - \left[\frac{\Sigma}{\Delta p}\int m_w \hat{c}_{nr}\ \delta \ell + \frac{\Delta p_o}{\Delta p}\int m_w \hat{c}_{nr}\ \delta \ell\right] , \tag{13}$$

The quantity $\delta M_w/\delta t$ is obtained by plotting a graph of M_w vs. time, drawing a smooth curve and evaluating the slope of this curve; alternately by taking the 24-hour change in M_w and applying this rate of change in the middle of the period with the assumption of linear change over 24 hours. This assumption, of course, may not hold so that the first method is to be preferred.

Precipitation Computation

For evaluation of the preceding equations the required quantities are the precipitable water content of the air and the velocity components normal and parallel to the direction of motion. The moisture content was obtained from the dewpoint curves of the radiosonde ascents (cf. fig. 6) by forming averages of specific humidity over layers of 100-mb thickness except for one layer of

variable pressure thickness from the surface pressure to the nearest 100-mb surface above the ground. Hand analyses were performed for each layer and for the total precipitable water content, illustrated in fig. 7. From such analyses values can be interpolated at the gridpoints of fig. 4.

Winds at each station also were averaged at first vectorially over layers of 100-mb thickness and over one layer of variable thickness near the ground, just as for precipitable water content. The lowest layer was adjusted to a 100-mb thickness by reducing the wind speed proportionately. For instance, if the thickness was 50 mb, speeds were halved, next, isogons and isotachs were drawn for each 100-mb thick layer to represent the fields of wind direction and speed. From these fields, plus the track of the center, the components u, v and u-c at the grid points of fig. 4 were determined.

After tabulation of all values the mass transports were computed for the four small boxes and also for the large box. The latter is shown for each computation period in fig. 8, while fig. 9 gives the mean for all periods. It is seen that in general lower inflow gave way to upper outflow, as is typical for cyclones. Above 400 mb winds were too strong and too few to permit reliable computation. Hence equations (3) and (11) were never properly checked. This is a distinct shortcoming which could be alleviated by choosing more recent cases since a marked improvement in operational wind measuring equipment and in methods of wind representation along the vertical (Riehl, 1961) have occurred since that time. Alternately, "composite" cyclones have been constructed from time to time from a number of cases to overcome the data shortage often present in individual cases. This technique, however, can serve only for first orientation and very likely would not be appropriate when cyclones move over variable terrain and on paths which always differ from case to case. In any event, the inadequate check on mass flow may be responsible for some of the shortcomings of the precipitation calculation.

From the mass flows and precipitable water content analyses the water vapor transports were computed, shown in the upper parts of figs. 8 and 9 for the large box. Inflow occurred throughout the lower troposphere during all four periods, with maximum in the layer 800-700 mb.

For evaluation of equation (13) M_w was averaged over each of the boxes from charts as illustrated in fig. 7. The quantity $\delta M_w/\delta t$ was obtained from a plot of M_w values in the (M_w, t) plane as already described. Finally, precipitation rate expressed in cm/12 hrs is shown in fig. 10.

Evidently, the calculation is not entirely stable because of the appearance of negative values, two of them rather large. To some extent, at least, this shortcoming may be related to the fact that method of analysis and computation were being developed. After establishment of a suitable routine of data processing, an improved result is likely to be achieved. The internal boundaries contributed a major share of the inconsistencies as may be seen when the precipitation for the large box is examined. For this box the amounts were 0.48, 0.28, 0.21 and 0.32 cm/12 hours, considerably more consistent in time than the amounts for the small boxes.

The precipitation amounts of fig. 10 are by no means negligible. Consider only the left front box which had the largest precipitation. The area of this box is 40,000 sq. mi. or about 26 million acres. Precipitation averaged close to an inch per day. Hence the water yield of the box is about 2 million acre-feet in 24 hours. Only half a dozen such days, when experienced over the Upper Colorado Basin, would account for the annual discharge at Lee's Ferry in a good water year of recent times.

It is of interest to compare the computed precipitation with that observed in rain and snow gauges of the area over which the cyclone travelled. This requires transformation from the moving to a locally fixed coordinate system, not an easy task. The method chosen was to permit the fixed stations to travel relative to the cyclone, hence to determine the water yield relative to the moving frame as indicated by these stations. Suppose that a gauge is situated on the forward cyclone boundary of fig. 4 at gauge reading time and that it travels to the rear edge in 24 hours. Then the gauge reading at the end of the period clearly must be the mean precipitation across the cyclone following the path of the gauge. Practical difficulties arise because the gauges initially are situated at many locations inside the cyclone and because they often pass beyond the rear boundary in 24 hours. If precipitation was measured at 12-hour intervals, this difficulty would be eliminated since the mean precipitation could be determined over much shorter path length. Alternately, given a very slow moving cyclone, many gauges would remain inside the boundary in spite of the 24-hour time interval for gauge reading.

Fortunately, the cyclone moved at moderate speeds so that a sufficient sample of gauges was available for a first approximation of precipitation as indicated by the gauges. Computational procedure was as follows. At first all observed precipitation amounts for the periods from 1 April 00Z to 2 April 00Z, and from 2 April 00Z to 3 April 00Z, were plotted using the Monthly Climatological Summaries. Stations reading precipitation more

than six hours different from 00Z were omitted. From the plotted charts mean precipitation values were obtained for small areas bounded by one-degree latitude and longitude (one-degree Marsden squares). These small areas were then moved relative to the cyclone. Those that remained located inside the large box for 18 and more hours were retained; the others were discarded. From the residual trajectories the precipitation as given by the gauge records was computed by summation. Comparable values were obtained from fig. 9 with the weighting formula

$P = 1/4 \left[P\,(03Z) + 2\,P\,(15\,Z) + P\,(03Z + 24) \right]$ for the precipitation rate.

The result of the comparison is given in fig. 11. This figure shows that calculated precipitation exceeded "observed" precipitation by about 50 per cent. The difference could be real and, if so, probably must be ascribed to unrepresentative location of the precipitation stations. In particular, there are few if any gauges at high altitudes where a large fraction of the precipitation often falls. This is an interesting possibility which needs to be investigated further by computations over a large data sample. For this purpose, a fixed coordinate system is more suitable than the moving one here employed. Computations of this type are planned as one sequel to the present study.

Further Analysis of Precipitation

It is evident that the left front box is of most interest in studying the precipitation associated with the cyclone. Hence the following comments will be confined to this area.

Dynamic Aspects: From inspection of figs. 1-2 the curvature of the 500-mb air current changes from cyclonic to anticyclonic across this area. This will be true also at still higher levels where wind speeds are much higher so that the air travels rapidly through the existing flow pattern. Assuming that the curvature change gives the sign of the change in the vertical component of vorticity about the earth's axis, we may apply the well known vorticity theorem

$$-(\mathrm{div}_2 V)_p = \frac{1}{(f+\zeta)_p} \frac{d}{dt} (f+\zeta)_p \qquad (14)$$

where $(\mathrm{div}_2 V)_p$ is the two-dimensional velocity divergence measured on an

isobaric surface, f is the Coriolis parameter, ζ the relative vorticity, and d/dt the time derivative following the mass. Since the absolute vorticity $f + \zeta$ may be assumed positive, it follows from (14) that a current which loses cyclonic vorticity must diverge laterally. Since surface pressure changes very little, mass continuity demands the presence of another layer with compensating convergence. This layer must be situated near the ground since the divergence is located in the high troposphere. Further, the lower converging air must ascend to the upper diverging layer from continuity reasoning. We have seen that mass and moisture flow is in accord with these deductions which are exactly the same ones that have been applied in cyclones of many geographical areas. Thus, broadscale dynamic analysis applied to a large precipitation region over the mountains does not appear to differ from that applicable to storms over flat land or over ocean. This is of interest in view of the difficulties often experienced in predicting precipitation over the mountain areas.

Thermodynamic Aspects: Examination of the temperature lapse rates around the cyclone showed that the most unstable air, with lapse rates in excess of the moist-adiabatic rate, was located in the left front box. Elsewhere, lapse rates were more stable with respect to moist adiabatic ascent and there were also inversion layers suggestive of subsidence.

Association of the main precipitation area with steep lapse rates not inhibitory to ascent, or even permitting buoyant ascent from the level of free convection, is a very interesting fact. When further the presence of various mountain chains within the area covered by the left front box at any time is considered, the following model of the ascending motion in the precipitation region may be advanced. Because of the near-buoyant condition ascent does not take place predominantly in broad sheets of stratus and altostratus, typical of warm front ascent in areas with lapse rate below moist-adiabatic. Rather, ascending columns cover only a small portion of the area of our box at any time, and ascent will be concentrated along the mountain ranges where an impulse toward upward motion is always present. Hence, in some ways, the situation may be hypothesized to be comparable with the narrow chimney ascent of the air moving into the tropical zone (Riehl and Malkus, 1958). There it was suggested that disturbed weather zones occupy 10 per cent of the whole tropical area; that active bands occupy 10 per cent of the regions with disturbance or one per cent of the equatorial area; and that within these bands most mass is funnelled upward in a small number of "hot towers" which occupy 10 per cent of the region with bands or only one per mill of the equatorial area. The last computation was based on approximate knowledge of size and vertical

draft speeds in cumulonimbus clouds. While exactly the same situation may exist in our active precipitation sector, we have no basis at present for taking such an extreme position. It is more probable that we should consider the middle scale mentioned as most significant for our computations, hence assume that active ascent takes place over about 10 per cent of the left front square with side of 200 n.mi.

With use of this model we wish to perform two computations with bearing on questions about precipitation structure and about the maintenance of the cyclone from the energetic point of view. Winter and spring precipitation concentrated along the high ranges, as contained in the model, occurs mainly in form of snow. Yet, from cloud observations one often finds a marked predominance of supercooled water cumuli over the ranges, with only occasional interspersed ice clouds. This suggests lack of sublimation nuclei effective at the temperatures of the clouds. On account of this situation some hope is thought to exist for artificial increases of precipitation through cloud modification, if it should be possible and worthwhile to inject sublimation nuclei active at the temperatures where supercooled water is observed. The present data can contribute to clarification of the value of cloud modification through computation of the levels and temperatures at which given percentages of condensation occur.

Consider fig. 12 which shows the air transport relative to the left front box, averaged over the four periods for which computations were made. The level of non-divergence was near 500 mb, with mass convergence below and mass divergence above 500 mb. Hence maximum upward mass transport took place near the 500-mb surface. Because of the steep lapse rate we may assume, for first approximation, that individual elements of the ascending mass conserve their identity and their equivalent potential temperature during the ascent which is quite rapid. The mass flow of 10^{13} g/sec at 500 mb corresponds to an ascent rate of 1 m/sec or 3.6 km/hr assuming upward motion is confined to one-tenth of the area of the box. Therefore we are concerned with upward displacements lasting on the order of one to three hours only, which supports the computational procedure to be followed.

This procedure is illustrated in fig. 13. At first the mean potential temperature and specific humidity, i.e. the equivalent potential temperature, was determined for the air entering the box in each layer of 100-mb thickness. Then each of these masses was permitted to ascend individually, and the path of each mass on the thermodynamic diagram was plotted, dry-adiabatic below the condensation level and moist-adiabatic above this level.

Assuming that condensation takes place at 100 per cent relative humidity, the condensate during ascent of 100 mb could be determined. After performing this calculation for each of the ascending masses -- with proportional deduction in the outflow layer above 500 mb -- the percentage of the total condensation product released in each layer of 100-mb thickness was found. These percentages are shown in fig. 14 where, however, the pressures have been replaced by the mean temperature of the whole ascending current at each level. This combination was permissible since the spread of temperature at each level was quite small.

Instead of computing the mass flow in 100-mb incremental steps it might have been better, though slightly more complicated, to determine it with respect to certain threshold temperatures, such as -20 C, at which temperature numerous types of freezing nuclei present in the atmosphere become active. Nevertheless, fig. 14 illustrates the result quite well. About 40 per cent of the condensation occurs below -20 C and 60 per cent at higher temperatures, where effective natural ice nuclei are scarce.

Further evaluation of this particular experiment with respect to possible uses of cloud modification is not possible. Variables, such as freezing of supercooled water on falling snow and the temperature to which the supercooled raindrops are carried, must be taken into account. It may well be that models involving these variables can extend the analysis, but this was considered beyond the scope of the present study. The preceding discussion mainly serves to show a method for computing the vertical distribution of percentages of condensate in relation to condensation temperature.

Release of Kinetic Energy

Various writers, notably Palmén (1958, 1962), have developed approaches for computing the release of kinetic energy in cyclones. While numerous physical processes contribute to growth, maintenance and decay of the energy of these systems, it is the release of potential energy through solenoidal circulations within the region of computation that is most relevant to our present inquiry. This release S is given by the sinking of cold relative to warm air expressed, following Palmén (1958), by

$$S = -\frac{R}{g} A \int \overline{\omega' T'} \, d \ln p \, . \qquad (15)$$

Here the bar indicates averaging over the area A and the primes denote deviations from the average. For determination of $\overline{\omega'T'}$ four values of ωT are available at each computation time, one in each of the four small boxes. Integrating from the surface to 300 mb and averaging over the four computation periods, values were obtained as depicted in fig. 15. A release actually occurred, i.e. ω and T were negatively correlated. The increase in kinetic energy of the cyclone due to this release amounted to 7×10^{19} ergs/sec or 6×10^{24} ergs/day. This value is very close to the actual kinetic energy present in our large box; hence the generation by solenoidal release was indeed substantial. In previous estimates in other cases the frictional dissipation of kinetic energy never amounted to much more than about 10 per cent of the total cyclone energy per day. These estimates, however, were made over flat land or over sea, not over rough and mountainous terrain. Therefore, without complete energy balance computation, it is not possible to establish a relation between generation and dissipation in the present case.

The contribution of condensation and sublimation heating to the solenoidal release is difficult to assess. The heat energy released during condensation and freezing, in the mean over the two days, was 10^{21} ergs/sec in mechanical units, or about 15 times larger than the solenoidal release. This value, however, has little meaning unless the efficiency of the thermodynamic system in converting heat to mechanical energy is known. In hurricanes, where almost the whole temperature field associated with these systems may be assigned to condensation heating, the efficiency is 2-3 per cent. In our case, the comparable amount would be 7 per cent. However, in middle latitude cyclones much, if not most, of the release comes through concentration of the pre-existing meridional temperature gradient into a narrow zone. Hence a simple statement about the contribution of condensation heating to production of kinetic energy cannot be made. Its most important function is to maintain or even slightly increase temperature in the rising portion of the storm with time. Without condensation, all ascent would be dry-adiabatic. In consequence of such ascent temperatures in the rising sector would rapidly cool by about 10 C in the middle and upper part of the troposphere. Since the temperature difference across the cyclone, observed on isobaric surfaces, also was of the order of 10 C, this temperature difference would soon vanish and the cyclone die if condensation stopped suddenly. From this consideration a qualitative argument in favor of an efficiency of 7 per cent for conversion of condensation heat to kinetic energy can well be put up. A precise computational framework, however, is lacking and its

development remains a task still to be undertaken. It may be that even over the Rockies, where a good moisture source frequently is lacking, the degree of cyclone development to be expected in any situation is not independent of the available moisture supply.

Acknowledgments

This report is based on one out of four problems taken up during a course entitled "The Atmosphere and the Water Cycle" offered during the winter quarter 1960 as an Advanced Subject Matter Institute under a grant from the National Science Foundation to Colorado State University. Most analyses were performed by Wm. M. Gray, Wm. E. Marlatt, J. E. Rasmussen and two Weather Bureau students attending the course, G. M. Krahl and O. J. Preikszas.

References

Bradbury, D. L., 1957, Moisture analysis and water budget in three different types of storms, J. Meteor., 14, 559-565.

Palmén, E., 1958, Vertical circulation and release of kinetic energy during the development of hurricane Hazel into an extratropical storm, Tellus, 10, 1-23.

Palmén, E. and E. O. Holopoinen, 1962, Divergence, vertical velocity and conversion between potential and kinetic energy in an extratropical disturbance, Geophysica, 8, 89-113.

Riehl, H. and J. S. Malkus, 1958, On the heat balance of the equatorial through zone, Geophysica, 6, 503-538.

Riehl, H., 1959, On production of kinetic energy from condensation heating. The Atmosphere and Sea in Motion, Rossby Memorial Volume. New York: The Rockefeller Institute Press, 381-398.

Riehl, H. and H. R. Byers, 1960, Computing a design flood in the absence of historical records. Geofisica Pura E Applicata, 45, 215-226.

Riehl, H., 1961, Quantitative representation of the velocity distribution along the vertical. Appendix to Borg Warner Controls Final Report to the Federal Aviation Agency, Santa Barbara Municipal Airport, Santa Barbara, Calif.

Sangster, W. E., 1960, A Meteorological coordinate system in which the earth's surface is a coordinate system, J. Meteor., 17, 166-176.

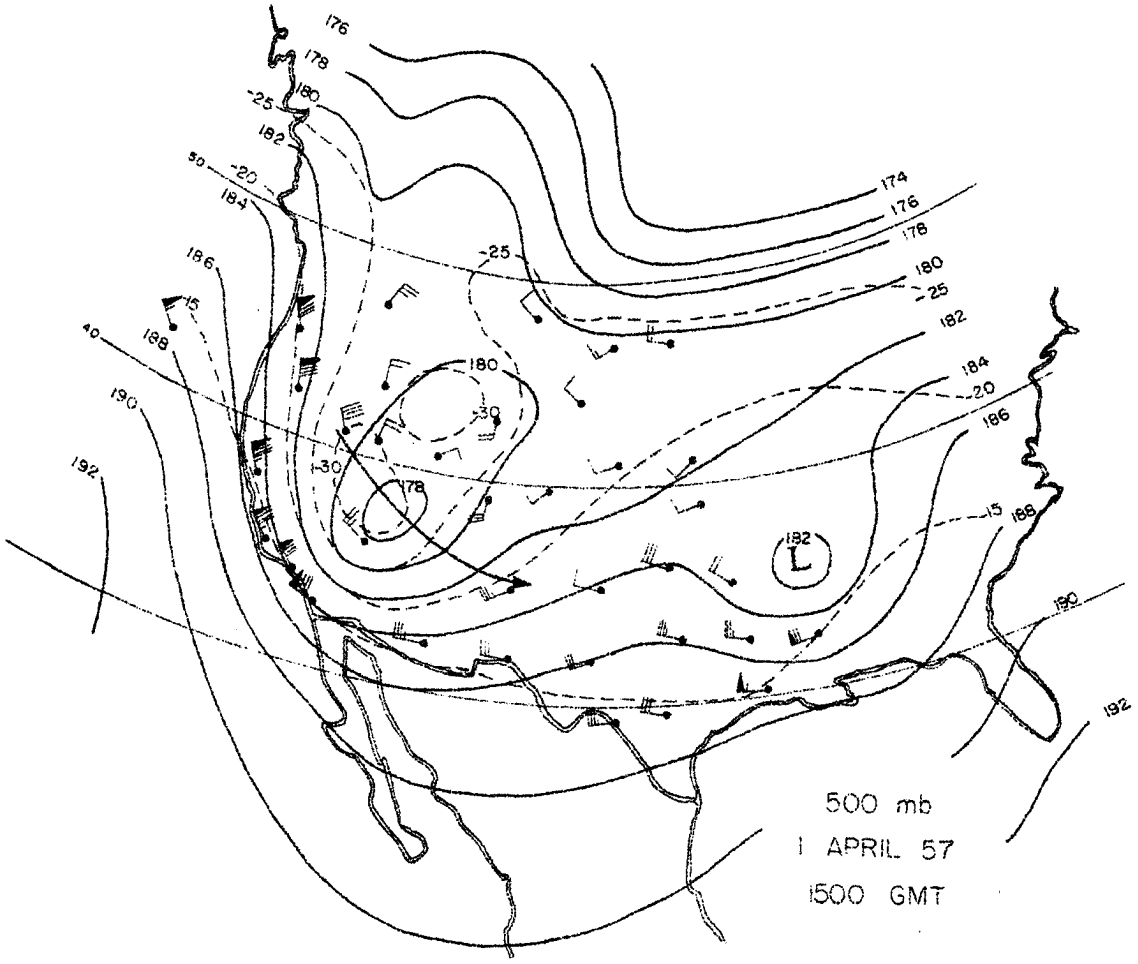

Fig. 1. 500-mb chart for 1 April 1957 1500 GMT. Location of rawinsonde stations for western United States shown. Analysis: height of 500-mb surface, 100's feet, solid lines; isotherms, deg. C, dashed lines. Curve with arrow denotes path of storm center analyzed. Wind observations: shafts from direction from which wind blows; a long barb denotes 10 knots, a short barb 5 knots and a heavy triangular barb 50 knots.

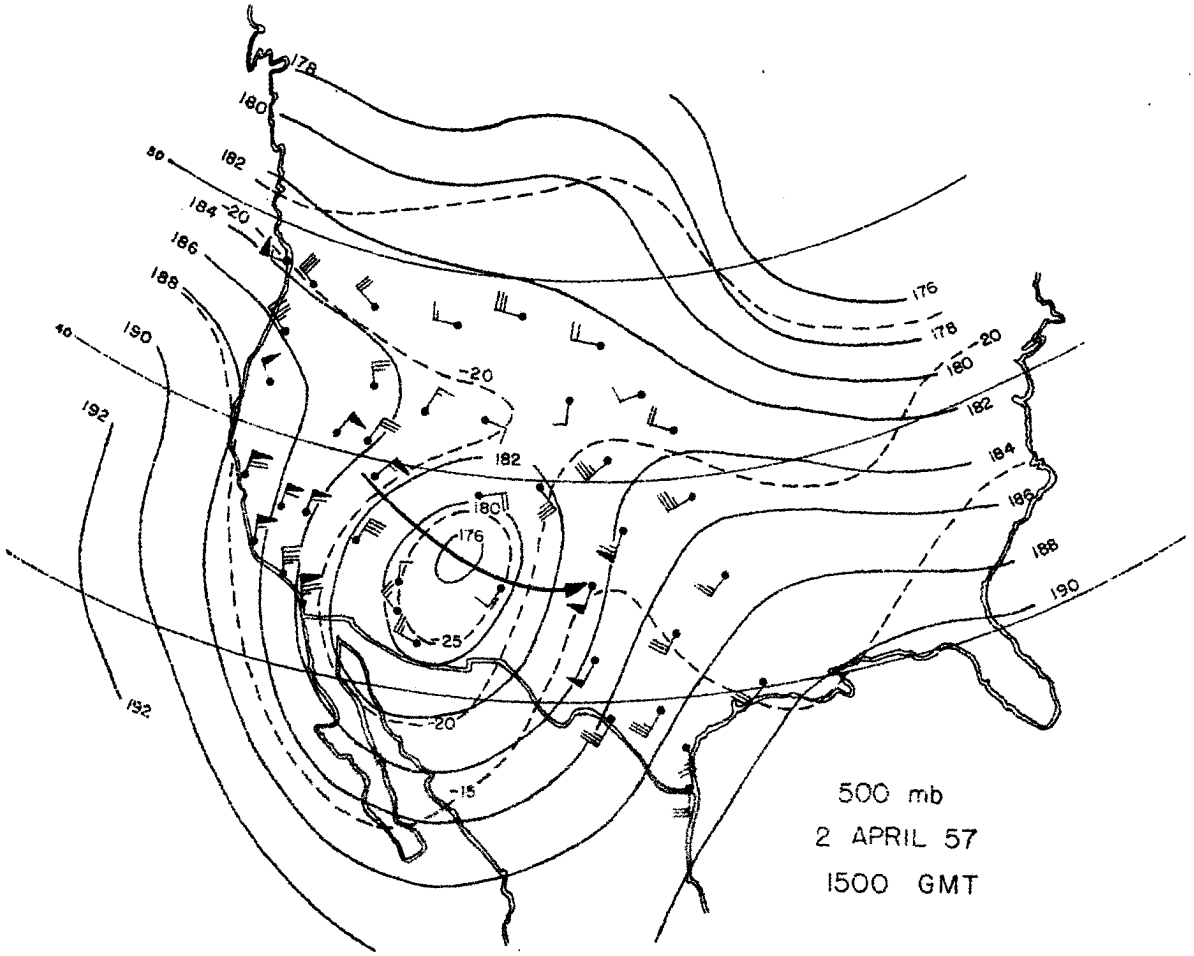

Fig. 2. 500-mb chart for 2 April 1957 1500 GMT. Notation as in fig. 1.

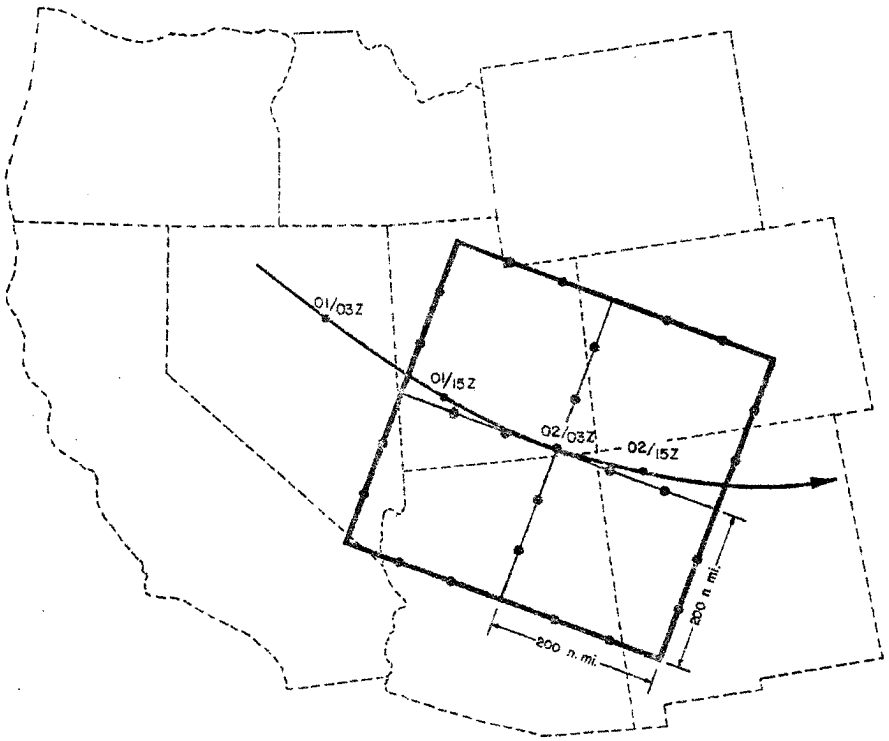

Fig. 3. State boundaries of western United States (dashed); path of 500-mb cyclone center during period analyzed from April 1, 0300 Z (GMT) to 2 April, 1500 Z, and computation grid placed geographically for 2 April, 0300 Z.

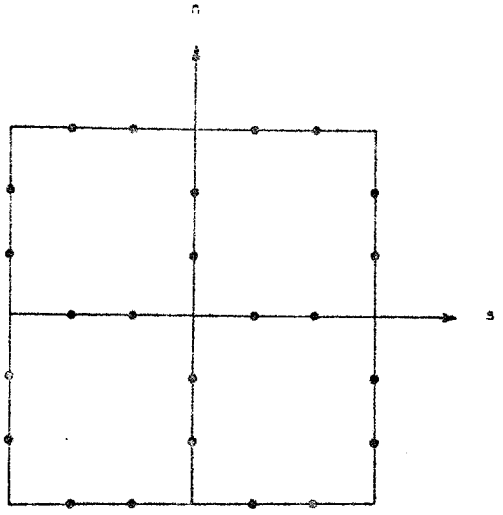

Fig. 4. Computational grid with s, n, coordinate system and points on boundary used for computations.

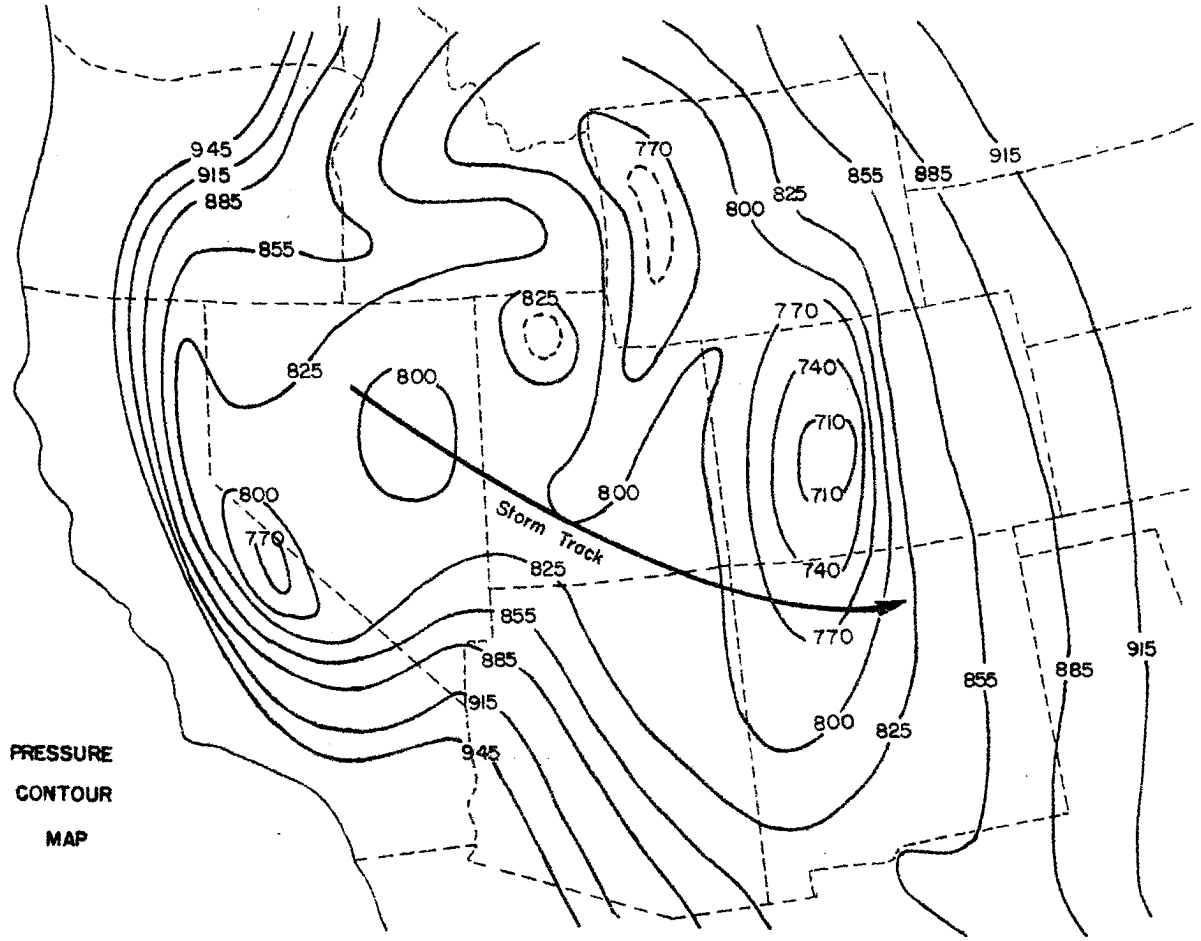

Fig. 5. Principal topography of western mountain area in pressure coordinate. Simplified topography from Sangster (1960).

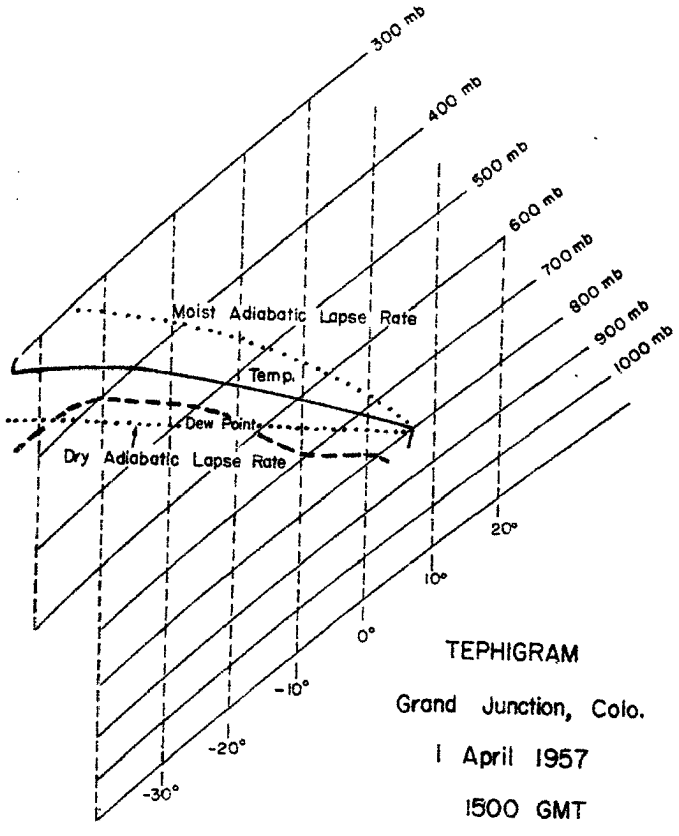

Fig. 6. Tephigram or the radiosonde ascent at Grand Junction, Colorado, 1 April 1957, 1500 GMT. Vertical lines are temperatures in deg. C.

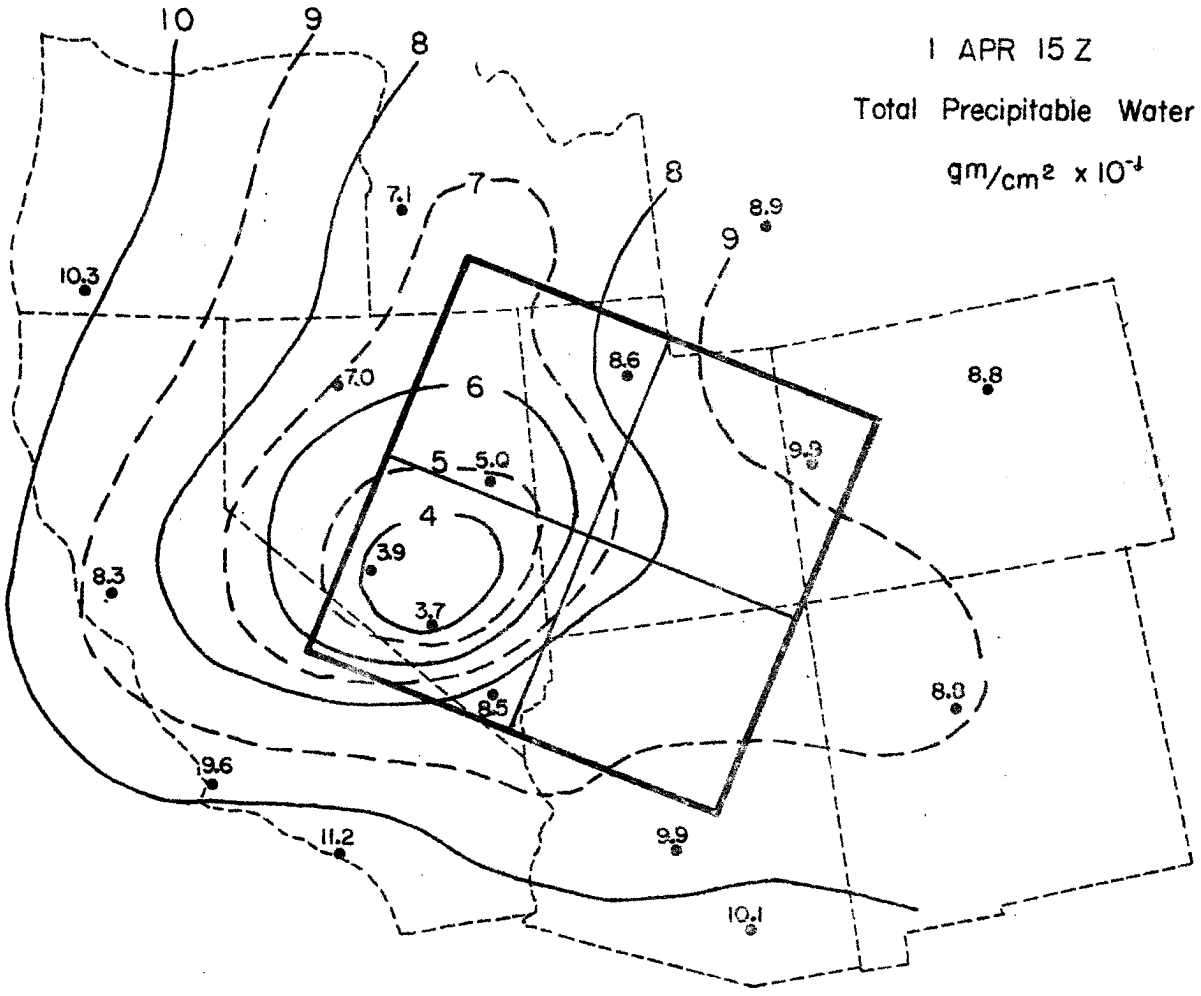

Fig. 7. Total precipitable water content of atmosphere (gm/cm^2), 1 April 1957, 1500 GMT.

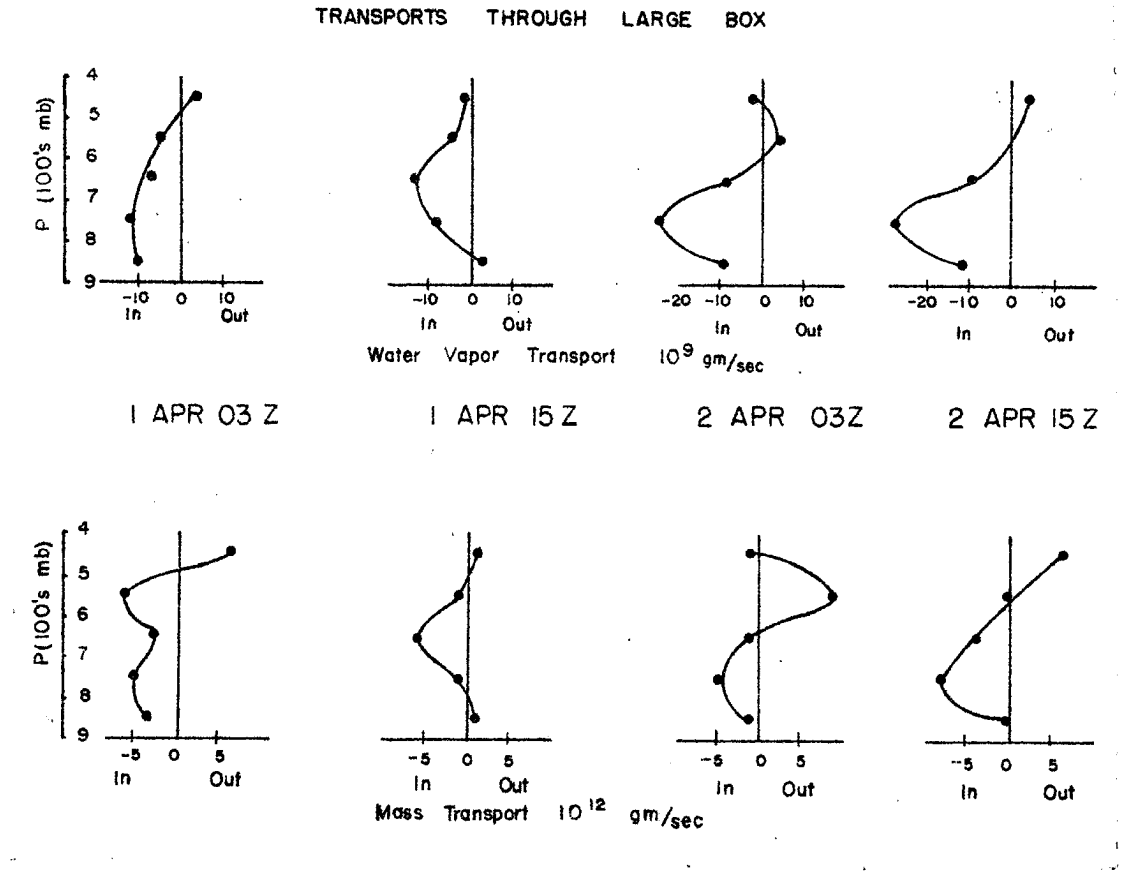

Fig. 8. Water vapor transport (upper row) and mass transport (lower row) through large box at the indicated times and with the indicated units.

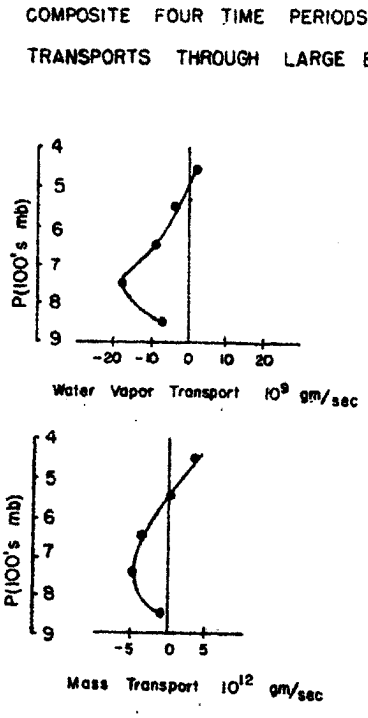

Fig. 9. Composite of fig. 8, all four periods combined.

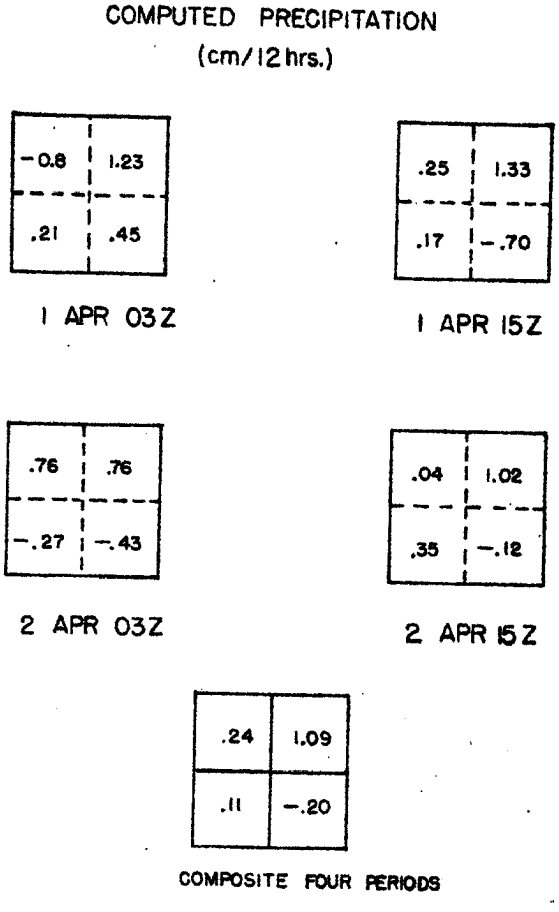

Fig. 10. Computed precipitation, expressed in cm/12 hrs, for each of the small boxes for the four computation times and for the composite of these times. Coordinate system attached to moving system.

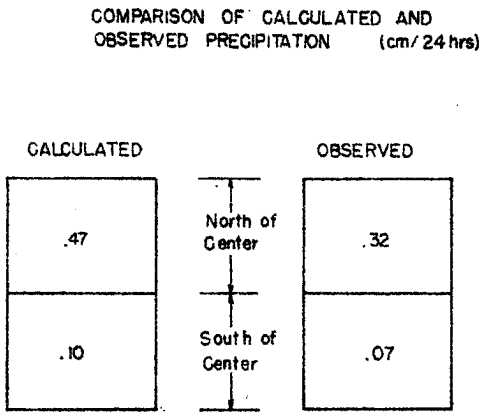

Fig. 11. Comparison of calculated and observed precipitation amounts for only those time periods when rain gauge stations were under the large reference box for more than 18 hours. Not to be compared directly with fig. 10.

Fig. 12. Mass flow through left front box, composite for four periods.

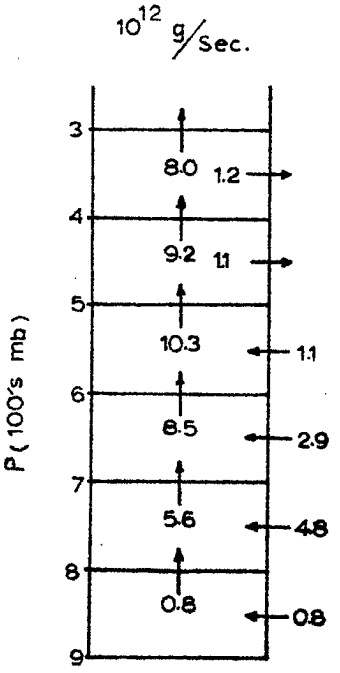

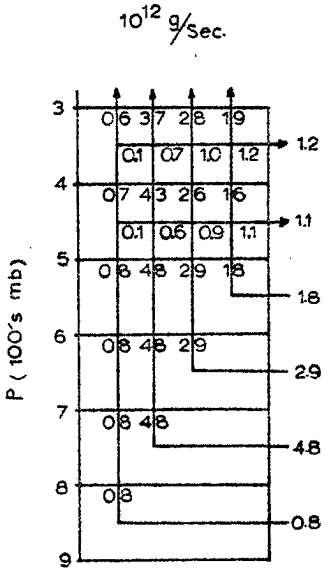

Fig. 13. Moisture transport through left front box computed according to scheme described in text. Number on outside (right) indicate inward or outward moisture flow; numbers along vertical lines indicate moisture transport in vapor form across each 100-mb surface; numbers along lateral lines inside box above 500 mb indicate accumulation of vapor flow from each vertical shaft to make up net outward vapor transport.

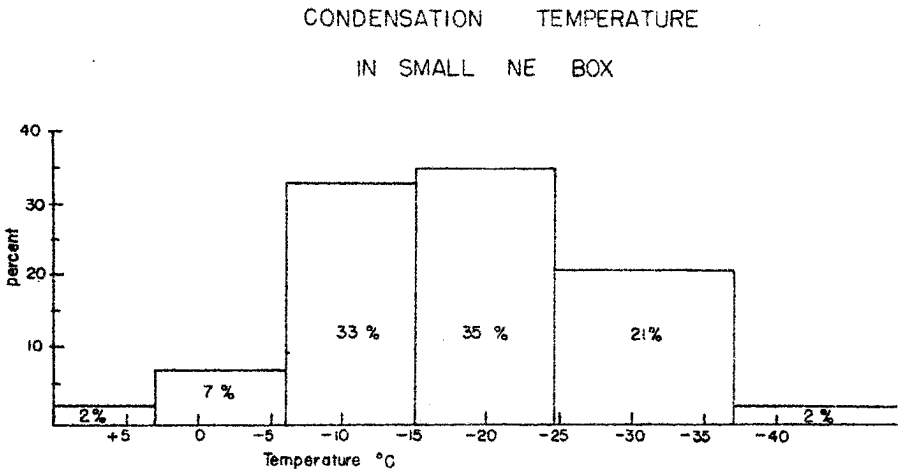

Fig. 14. Per cent of condensate related to temperature at which condensation was computed to occur.

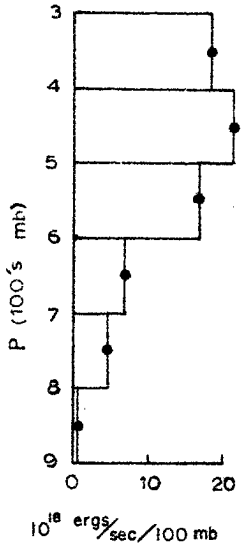

Fig. 15. Release of kinetic energy (10^{18} ergs/sec/100 mb) in each layer of 100 mb thickness for large box, all four periods combined.